available at www.sciencedirect.com

ScienceDirect

www.elsevier.com/locate/brainres

BRAIN RESEARCH

Research Report

Consequences of parameter differences in a model of short-term persistent spiking buffers provided by pyramidal cells in entorhinal cortex

Randal A. Koene[*,1], *Michael E. Hasselmo*[1]

Center for Memory and Brain, Department of Psychology and Program in Neuroscience, Boston University, 64 Cummington Street, Boston, MA 02215, USA

ARTICLE INFO

Article history:
Accepted 12 June 2007
Available online 17 July 2007

Keywords:
Short-term memory
Sustained spiking
Theta rhythm
Parameter selection
Working memory capacity
Entorhinal cortex activity

ABSTRACT

In previous simulations of hippocampus-dependent and prefrontal cortex-dependent tasks, we demonstrated the use of one-shot short-term buffering with time compression that may be achieved through persistent spiking activity during theta rhythm. A biophysically plausible implementation of such a first-in first-out buffer of short sequences of spike patterns includes noise and differences between the parameter values of individual model pyramidal cells. We show that a specific set of parameters determines model buffer capacity and buffer function, and individual differences can have consequences similar to those of noise. The set of parameters includes the frequency of network theta rhythm and the strength of recurrent inhibition (affecting capacity), as well as the time constants of the characteristic after-depolarizing response and the phase of afferent input during theta rhythm (affecting buffer function). Given a sufficient number of pyramidal cells in layer II of entorhinal cortex, and in each self-selected category of pyramidal cells with similar model parameters, buffer function within a category is reliable with category-specific properties. Properties include buffering of spikes in the order of inputs or in the reversed order. Multiple property sets may enable parallel buffers with different capacities, which may underlie differences of place field sizes and may interact with grid cell firing in a separate population of layer II stellate cells in the entorhinal cortex.

1. Introduction

Models of hippocampal and prefrontal cortex function used in simulations of many behavioral tasks need a short-term buffer that does not depend on synaptic modification. Simulated episodic encoding of spike patterns in recurrent networks often relies on spike-timing-dependent potentiation (Bi and Poo, 1998) with Hebbian learning characteristics (Hebb, 1949). Such a sequence learning protocol requires repeated and ordered presentation of successive stimuli with regular small time intervals (less than 40 ms). Short-term buffering of a sequence of input and multiple subsequent cycles of retrieved spiking activity at appropriate time intervals can provide a buffer for this synaptic encoding.

Synaptic modification is not a plausible mechanism through which to buffer a single presentation of the input, but an

* *Corresponding author*. Center for Memory and Brain, 2 Cummington Street, Boston, MA 02215, USA. Fax: +1 928 543 5112.
E-mail address: randalk@bu.edu (R.A. Koene).
URL: http://rak.minduploading.org (R.A. Koene).
[1] Fax: +1 617 353 1424.

0006-8993/$ – see front matter © 2007 Elsevier B.V. All rights reserved.
doi:10.1016/j.brainres.2007.06.067

intrinsic mechanism that elicits persistent spiking in response to input is feasible. An after-depolarizing (ADP) membrane current in pyramidal cells of layer II of entorhinal cortex enables intrinsic persistent spiking (Klink and Alonso, 1997a,b; Egorov et al., 2002). The after-depolarization and persistent spiking appear to be most prominent in layer II pyramidal cells, and do not appear in layer II stellate cells (Klink and Alonso, 1997b). In contrast, layer II stellate cells exhibit subthreshold membrane potential oscillations (Klink and Alonso, 1997b) that differ in frequency along the dorsal–ventral axis and may underlie firing in a grid like pattern (Giocomo et al., 2007). Models of short-term memory based on interactions of after-depolarization and theta rhythm have been studied in simulations by Lisman and Idiart (1995) and Jensen et al. (1996), as well as in our own work (Koene et al., 2003; Koene and Hasselmo, 2005, 2007).

Our integrate-and-fire model of short-term buffering generates an asymmetric distribution of spiking activity within each cycle of the theta rhythm (Koene et al., 2003) that enables phase-locked integration of buffer intervals of acquisition and retrieval with intervals of encoding and retrieval in connected networks, as well as a plausible mechanism for the first-in first-out (FIFO) ordered replacement of items that are maintained in the buffer (Koene and Hasselmo, 2007). The model was used to simulate performance in hippocampus-dependent spatial navigation tasks (Hasselmo et al., 2002; Koene et al., 2003) and in tasks that depend on temporal context-dependent episodic memory (Koene and Hasselmo, 2006b). A limited buffer capacity and the first-in first-out replacement of items are a good fit to the recency portion of graphs of serial position data (Atkinson and Shiffrin, 1968; Kahana, 1996), and psychophysical evidence of ordered item displacement has been gathered in tests ranging from precategorical acoustic storage (Crowder and Morton, 1969) to the observed interaction between memory load and item position for semantic information (Haarmann and Usher, 2001).

Entorhinal cortex layer II (ECII) is the major source of input to the hippocampal system. Pyramidal neurons in ECII exhibit after-depolarization (ADP) following spikes (Klink and Alonso, 1997b), and membrane potentials in both the entorhinal cortex and hippocampus are modulated at theta rhythm, due to input from the medial septum. Combined rhythmic modulation and ADP may be used in a mechanism that sustains regular persistent spiking, a sequence buffer first proposed by Lisman and Idiart (1995). In prior work, we demonstrated an integrate-and-fire model of a short-term spike buffer in ECII that is based on these properties (Koene and Hasselmo, 2007). If short sequences of spiking patterns are sustained in ECII then these time-compressed and repeated representations of a behavioral episode can elicit significant synaptic potentiation in hippocampal recurrent networks (Koene et al., 2003).

A constrained set of biophysical requirements follows from the general principles of the working buffer:

- ADP rise and fall time constants ($\tau_{rise,ADP}$, $\tau_{fall,ADP}$) must be (a) sufficiently large so that the ADP manages to return a neuron's membrane potential to threshold on the rising flank of depolarization by theta rhythm, and (b) small enough to allow persistent spiking to be terminated by a limited interval of inhibitory input. Ideally, rise and fall time constants are each similar to the duration of a theta cycle. Experimental results by Klink and Alonso (1997b) and simulation studies by Fransén et al. (2002) suggest time constants that differ significantly from initial versions of our model. We attempt a first analysis of the effect of this difference here.
- Afferent input must appear within specific phase intervals of the theta cycle, which enables ADP to achieve the first repetition of new item spiking either (a) within the same theta cycle for a forward-order buffer, or (b) as the first item reactivation on the depolarizing flank of the next theta cycle for an order reversing buffer. These input intervals must be separated from the theta interval in which sustained buffer activity reappears to avoid interference between buffered spike patterns and novel input.
- A network of interneurons must supply adequate recurrent inhibition to neurons in the buffer in response to buffered item spikes, so that a minimum time interval between the spikes of successive item representations is enforced. The inhibitory mechanism of item separation also supports continued temporal coherence between the spikes of neurons that represent one item without relying on strengthened connections between those neurons.

We hypothesize that natural conditions of short-term buffering in ECII include variations of the values of this set of critical model parameters in individual neurons, as well as additive noise (White et al., 2000). Here we demonstrate first-in-first-out buffer function in the noisy case, at different frequencies of the network theta rhythm or of network-wide recurrent inhibition, and in cases of individual differences between parameter values for (i) the characteristic amplitude and time-constant of after-depolarization (ADP) and (ii) the neuron-specific strength of recurrent inhibitory input.

Within the neural circuitry of the buffer, model parameters of the neurons and their connections must fall within a similar range that allows them to function together to hold one item in the persistent spiking buffer. This is a general principle of self-selection during one-shot acquisition of a novel item input with a representative pattern of spiking buffer neurons. Where there are differences between the parameters of pyramidal neurons in ECII, we show that those may affect reliable buffer function and may affect the capacity of the buffer. Differences between individual neurons have two main consequences: (1) Neurons with similar model parameter values form subsets or categories. Within a subset, neurons can function as successful components of a persistent firing buffer with characteristics specific to the subset of neurons. (2) A persistent spiking neuron can drop out of the representation of a specific buffered item, thereby reducing the ensemble size of the neural representation. This second consequence is also a common outcome of significant noise. Parameter and noise related consequences are mitigated when large ensemble sizes are used to represent each buffered item. We speculate that the existence of different subsets may lead to effective buffering of sequence input in multiple buffers with different characteristics, such as buffering with repetition in the same order as input is received or with repetition in the reversed order.

2. The model

In a previous work, we demonstrated the usefulness of our working buffer model in simulations of hippocampus guided

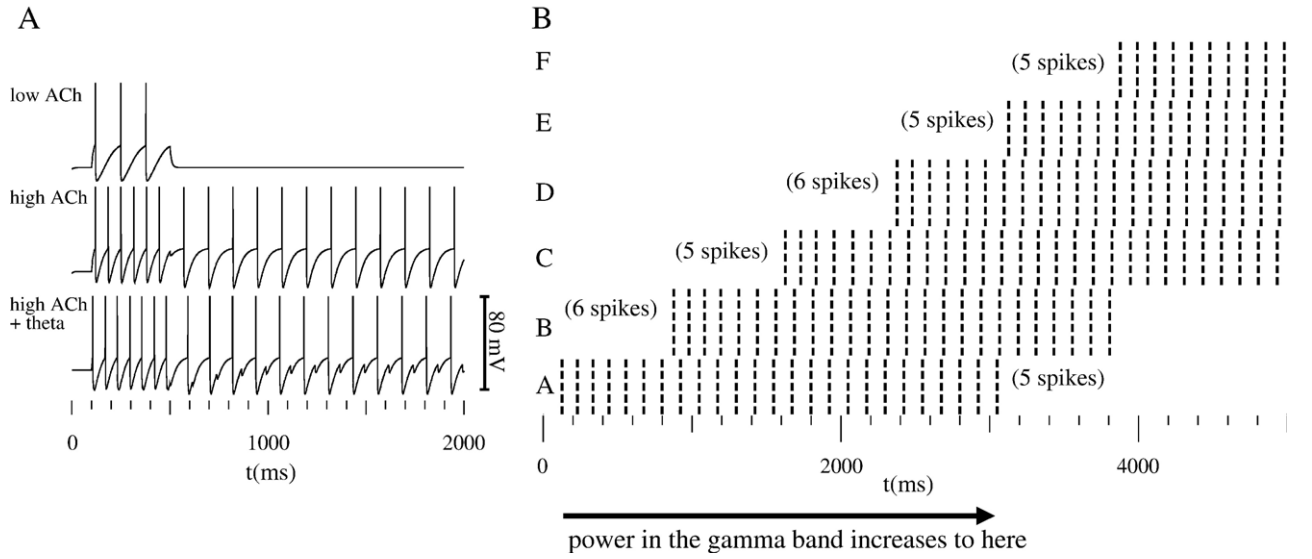

Fig. 1 – Short-term buffering based on persistent spiking. (A) Model responses of the cholinergically modulated after-depolarization (ADP) of a pyramidal neuron in layer II of the entorhinal cortex. Injecting current over 400 ms at low levels of acetylcholine (ACh) causes transitory spikes. At high levels of acetylcholine, repetitive spiking of the pyramidal neuron persists at a rate determined by the time course of ADP. When we include the effect of modulated membrane potential at theta rhythm, persistent spiking occurs regularly at the same phase of the theta cycle. (B) Short sequences of patterns of simultaneous spikes are sustained by the buffer. Spiking representations of items A to F, consisting of five or six spikes each (a total of 32 spiking neurons), enter the buffer at successive onset times. Buffered spike patterns are reactivated in their order of acquisition during each theta cycle. The spiking representation of A is terminated as E appears, and B is terminated as F appears, demonstrating first-in-first-out queuing with a capacity for sequences of four spiking patterns.

spatial navigation (Koene et al., 2003) and of goal-directed behavior in PFC (Koene and Hasselmo, 2005). Depictions of our short-term buffer model and examples of modeling with Catacomb are included in Cannon et al. (2003). In Koene and Hasselmo (2007), we contrasted our model with other models of working memory and described its kinship to the earlier persistent spiking buffer model by Lisman and Idiart (1995), which was used extensively by Jensen, Idiart and Lisman (1996). Our model extended that earlier work by specifying a more plausible simulation of theta modulated membrane potential, by specifying a neural mechanism that enables the representation and first-in-first-out replacement of items represented by different spiking ensemble sizes, and by demonstrating usable buffer function in the presence of noise. We will describe the effects of different model parameter settings, especially in the context of the reverse order buffering version of the model. A reversing buffer can be used to establish backward or bidirectional episodic associations. This capability is particularly relevant, since recent electrophysiology in spatial navigation tasks has shown that both forward and reversed retrieval of sequences of activity occur in the hippocampus (Foster and Wilson, 2006; Johnson and Redish, 2006).

After-depolarization (ADP) is assumed to elicit persistent firing in our model of short-term memory in ECII. ADP has been observed following spikes in the presence of cholinergic modulation in ECII pyramidal neurons (Klink and Alonso, 1997b; Fransén et al., 2002), as well as in pyramidal neurons of the prefrontal cortex (Andrade, 1991). Fig. 1A shows persistent firing effects of ADP at low and high levels of acetylcholine, and with the addition of rhythmic theta oscillation (Acker et al., 2003). During a modeled period of short-term buffer function, we presuppose a response at saturation levels of the ADP, so that after each spike the membrane potential resets and then ramps up with the same amplitude and time constant.

The buffer mechanism previously described (Koene and Hasselmo, 2007) specifies that the response of leaky integrate-

Fig. 2 – The membrane response of one neuron in each of the item representations A to F, during spike buffering in order and during item replacement. The simulation included a population of 29 persistent firing pyramidal neurons, of which subsets of two to eight spiking neurons represented individual items. (A) Four items are buffered before replacement occurs. The membrane response of each neuron exhibits spikes at order-specific phases of rhythmic buffer cycles, as well as subsequent hyperpolarization and the onset of an after-depolarizing response. (B) The expanded time scale of a small section of the simulation output shows buffer reactivation and item replacement. Recurrent "gamma" inhibition causes hyperpolarizing dips of pyramidal membrane potentials throughout the network at regular intervals that follow each spiking pattern. The spikes of consecutive reactivated spike patterns are separated by an interval small enough, so that spike-timing-dependent potentiation (STDP) can be elicited in associative networks that receive the output of the buffer. "Replacement inhibition" elicited by a neural mechanism for first-in-first-out item replacement appears at the onset of buffered spike reactivation when input appears in a full buffer.

and-fire model ECII pyramidal neurons is affected by membrane currents that are characterized by individual values of conductance (g_i) and reversal potential ($E_{rev,i}$). The post-synaptic and intrinsic currents are modeled by double exponential functions (see Appendix A) for: a membrane leak current, regular input responsible for modulation at theta rhythm that originates in the medial septum, afferent stimulus input to the buffer, intrinsic after-hyperpolarizing and after-depolarizing responses to action potentials, and inhibitory synaptic input from the recurrent fibres of an interneuron network that is responsible for observed modulation at gamma frequency (25–50 Hz). A spike depolarizes the membrane to 0 mV. A characteristic membrane capacitance

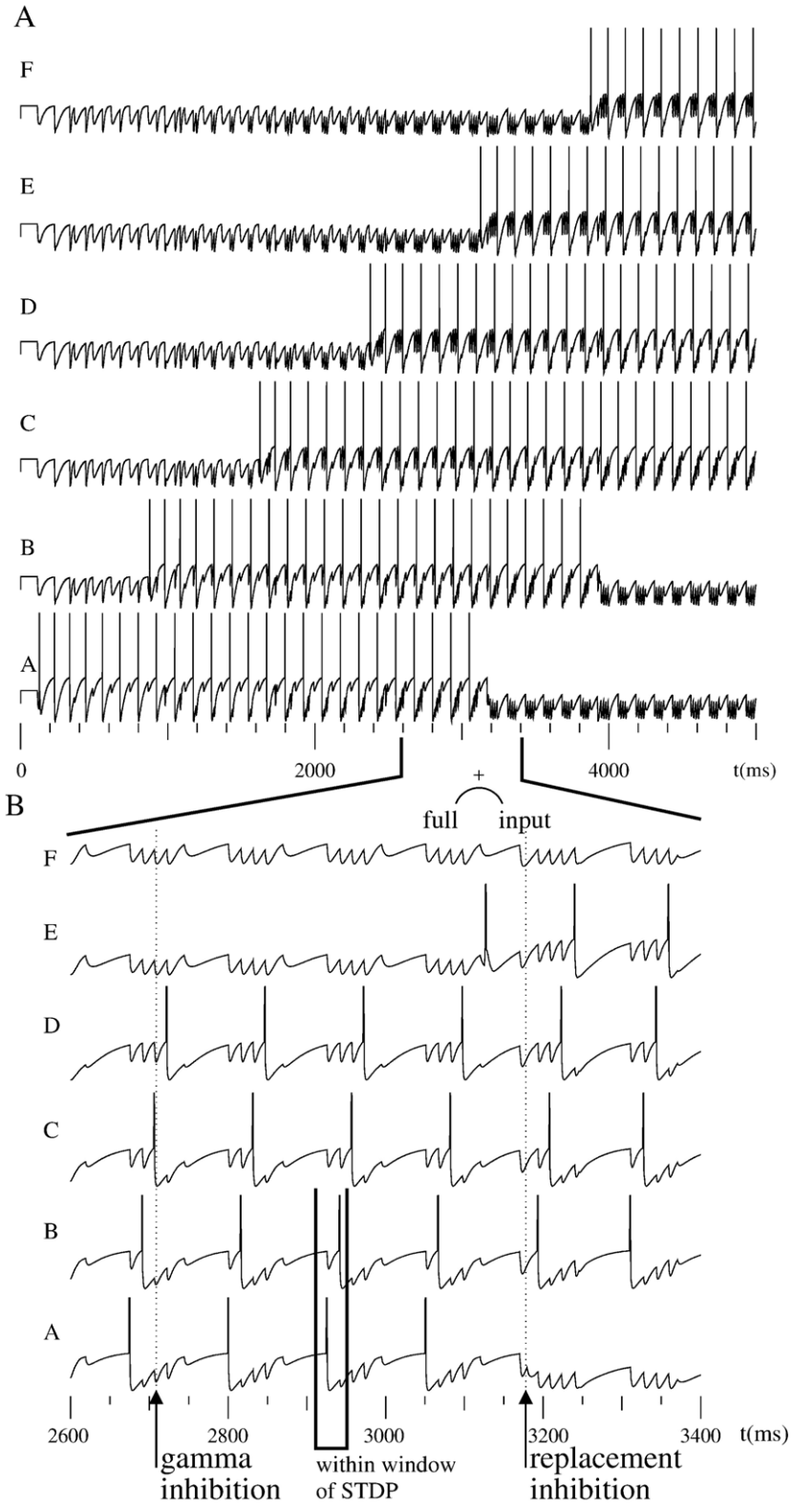

and leak current determine the time course of an exponential decay of membrane potential to a characteristic resting potential.

Buffered items are represented by patterns of simultaneous spikes, which are repeated rhythmically at theta frequency (3–12 Hz). These regular cycles established through the rhythmic modulation of buffer neurons by septal input contain asymmetric intervals of buffered activity (on the depolarizing flank of theta modulation) and of afferent input to the buffer (Jacobs et al., 2007). Our model aims to present the realistic membrane response to theta modulation. Recurrent inhibition believed to be responsible for observed gamma oscillations (25–50 Hz) maintains the ordinal separation of successive buffered items, as an interneuron network is activated by buffer spikes (Lisman and Idiart, 1995).

Non-overlapping spiking representations require one or more pyramidal buffer neurons for each of the items presented during a simulation. The number of spiking neurons that represent different items presented during a simulation need not be the same. To produce the simulation results shown, we used two to eight spiking pyramidal neurons to represent an item and a single model interneuron to represent inhibitory activity generated by the network-wide activation of an interneuron network. The response of the model interneuron does not exhibit after-depolarization.

Our proposed mechanism for first-in first-out (FIFO) replacement of items in a buffer that queues items in the ("forward") order of experience (Koene and Hasselmo, 2007) does not depend on the number of spikes that represent a buffered item or that represent a novel input, as shown in Fig. 1B, in which each item is represented by either five or six spiking neurons of a population of 32 model pyramidal neurons. Item replacement is both triggered by and targeted to the theta phase of buffered spikes. A description of the responses and interactions of neurons involved in the proposed mechanism is included in Appendix A.

Input to specialized subsets of pyramidal neurons is modulated by theta rhythm, such that one subset is activated in response to buffer neuron spikes that occur at the theta phase during which the last buffered item is reactivated in a full buffer (designated in Appendix A as "Pf " neurons). Another subset is activated in response to novel input to the buffer (designated in Appendix A as "Pi" neurons). When both the full buffer and input detecting neurons spike, phase-locked activity is elicited in a set of interneurons (designated as "Ir" interneurons in Appendix A) that deliver "replacement inhibition" to the persistent firing pyramidal neurons of the buffer. Fig. 2 shows the membrane responses that the mechanism elicits in persistent firing pyramidal neurons during simulated buffering and replacement of six items. One membrane response curve is shown for each of the items A to F, which were represented in the simulation by 5, 2, 8, 4, 3, and 7 spiking neurons, respectively.

At the first item reactivation phase, the degree of depolarization by theta modulation and the ADP response of the persistent firing pyramidal cells are tuned, so that the firing threshold can be reached only at that phase, where the combination of theta modulation and ADP is maximal for those neurons involved in the item representation. At that phase, replacement inhibition suppresses spiking and consequently terminates persistent firing of the neurons that were used for the spiking representation of the first item. Subsequent buffered item spikes shift to earlier theta phases and are followed by repetition of the spike pattern that represents a new buffered item (Fig. 2). The capacity of the buffer model is adjustable by modifying the phase at which spiking can be elicited in the full buffer signaling neurons (Pf neurons in Appendix A), up to a maximum imposed by the number of gamma cycles that fit into the reactivation interval of each theta cycle.

In tasks such as delayed spatial alternation, which require temporal context-dependent episodic memory, an order reversing buffer can achieve one-shot acquisition of a sequence. Repetition of spike patterns in the reverse order of the corresponding experience enables spike-timing-dependent potentiation (STDP) of synapses in hippocampal recurrent networks and hippocampal associative retrieval in the reversed order, as recorded in recent experiments (Foster and Wilson, 2006), which can retrieve events in a preceding temporal context and enable correct decision making in the behavioral task (Koene and Hasselmo, 2006a, b). Our implementation of the reversed order buffer differs from that of the forward order buffer in two ways: (1) A different phase offset of afferent input results in order reversal, since novel spikes are repeated as the first spike pattern during the next theta cycle. (2) First-in first-out queuing in the reversing buffer requires no explicit mechanism to achieve correct item replacement. Fig. 3 shows reversed order buffering of six items that were each represented by subsets of five or six spiking neurons from a simulated population of 32 pyramidal cells.

As the membrane response traces in Fig. 3 show, even though the reactivation order of item spikes in the buffer is reversed, the network still functions as a first-in first-out buffer, since the earliest item buffered (A in Fig. 3) is also the first item to be terminated when new input (F in Fig. 3) enters the full buffer. In the reversed order buffer model, pattern separating recurrent gamma inhibition shifts the reactivation of earlier items into later phases of the theta cycle when the reactivated spikes of new input appear first in the buffered sequence. Once shifting is completed in a full buffer, the new reactivation phase of earliest item spikes falls into the hyperpolarizing interval of the theta modulation. That terminates the persistent firing. In order to test the effects of individual parameter differences between model ECII neurons, we constructed a grid of independently modifiable buffer neurons in the Catacomb model.

3. Results

In our previously demonstrated default configuration of the buffer model (Koene and Hasselmo, 2007), we achieved robust buffer function with gamma intervals of item separation that enables spike-timing-dependent potentiation (STDP) in the presence of noise (Fig. 4). Although the effects of noise on a neuron's membrane potential may affect the timing of a spike, this drift is countered by the recurrent inhibition, which promotes coherence. Eventually, drift of spike times causes participating neurons to drop out of the buffered persistent spiking, but without interfering with the sequence order of buffered items. Maintaining the order, even as item

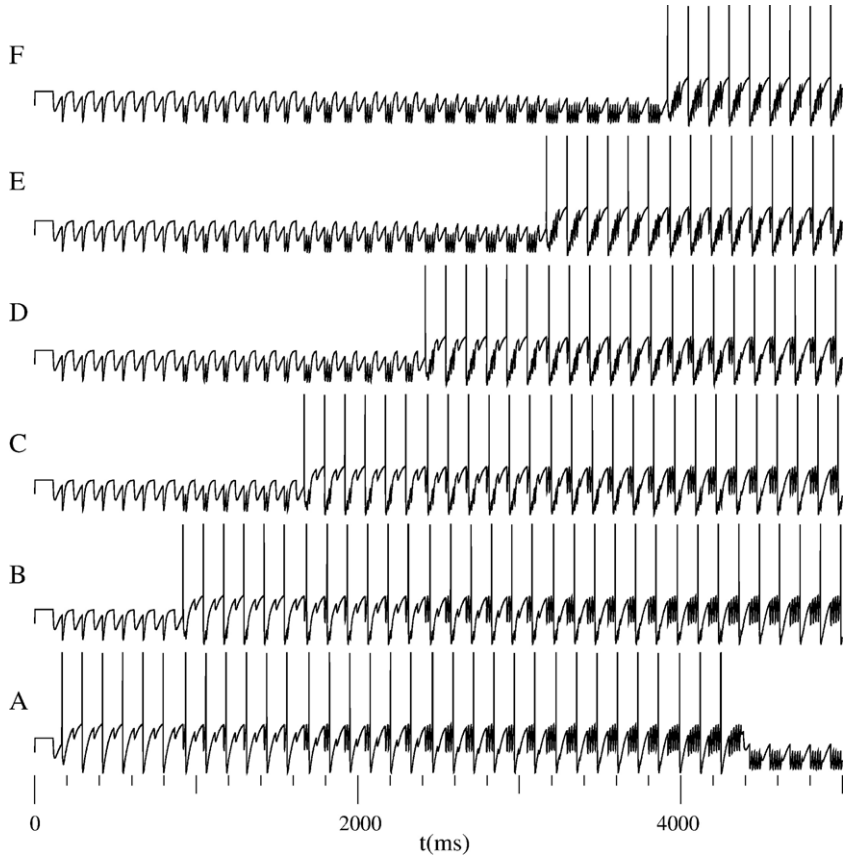

Fig. 3 – The membrane potentials of one neuron in each of six item representations (A to F), sustained in a reversed order buffer. During the simulation, each item was represented by a subset of five (A, C, E, F) or six (B, D) spiking neurons from a population of 32 model pyramidal cells. The buffer model uses no explicit item replacement mechanism, but demonstrates five item capacity in this simulation.

expression is weakened in proportion to an item's age in the buffer, is a useful property that can support reliable episodic encoding.

The present implementation of the ECII model retains the same buffer performance, even though it no longer includes phasic modulation that was used in our earlier implementation

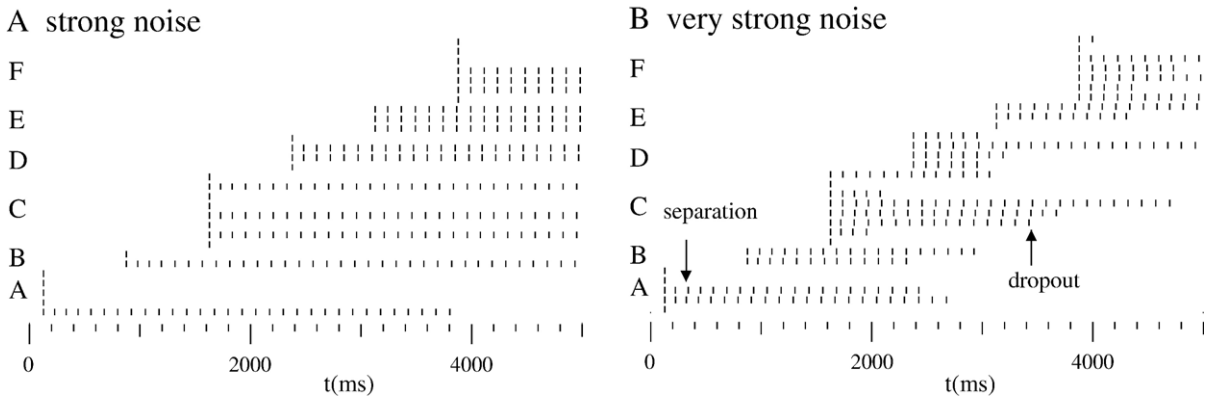

Fig. 4 – Simulations with noise in the model of six buffered items (A to F), each represented by spike patterns that initially elicit between two and eight spikes (total of 29 spiking neurons). Sustained spiking at low levels of noise is shown in Fig. 1B. (A) At strong noise levels, an initial selection of spikes that reactivate in the same gamma interval is sustained for each item representation (13 of the 29 neurons). (B) When noise levels are elevated further, those representations exhibit separation into adjacent gamma intervals and a gradual drop out of spikes (examples indicated by "separation" and "drop-out" arrows). Despite the separation of spikes in each pattern, the order of spikes sustained for consecutive items was not violated in these simulations, so that the order of item representations in a buffered sequence was maintained.

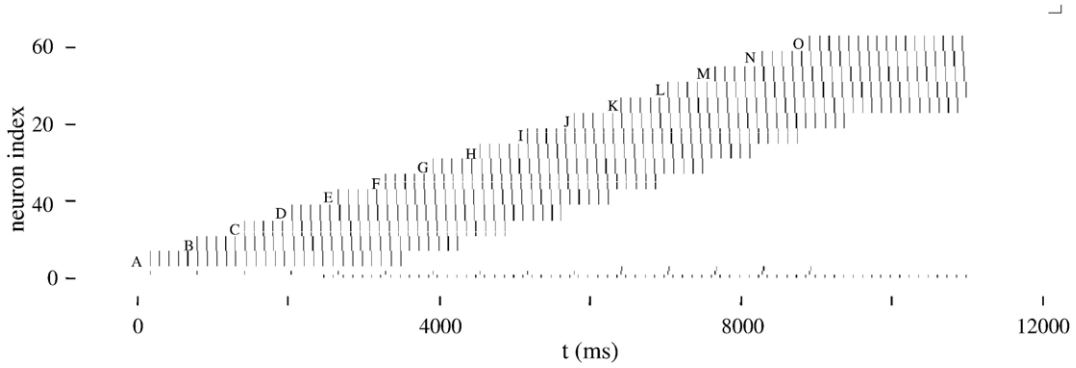

Fig. 5 – Correct reversed buffer spiking for 15 items (A to O) represented by 4 spiking neurons per item, with a buffer capacity of five items (e.g. K, L, M, N, O). The simulated buffer model did not utilize transmission modulation to regulate afferent and recurrent activity.

(Koene and Hasselmo, 2007) to suppress transmission of afferent input when buffered spikes are reactivated and to suppress recurrent inhibition during the input interval of each theta cycle (Fig. 5). This was expected: Circuitry regulating the input ensures that input spikes appear only at the designated input phase, and that phase is sufficiently separated from the phase of the first buffered spike, so that recurrent inhibition due to spikes elicited by afferent input has no effect.

Buffer function depends entirely on the ADP response in our model. A rise time constant that is significantly less than the duration of a theta cycle does not enable spike reactivation at theta rhythm. In contrast, a time constant that is too long has the potential to disrupt the timing of individual buffer items. We explore the effect of larger rise time constants, specifically an ADP response that can affect more than two theta cycles. Due to the reset of ADP following each spike, the extended intrinsic response to after-depolarization with greater time constants did not affect simulated maintenance of buffered items. Fig. 6 shows the membrane responses of five buffered items during a simulation with a sequence of 15 input items. Each item was represented by four spiking neurons from a population of 60 model pyramidal cells. A forward order buffer model with increased ADP rise time constant does require a stronger replacement inhibition to terminate persistent firing of the oldest item.

Increasing the rise time constant of ADP can decrease robustness of the buffer in noisy conditions. Strong ADP at intervals greater than one theta cycle can allow spiking, even if the spike time has been shifted significantly by noise. Instead of merely weakening item representations in which shifted spikes drop out, buffered item representations may overlap and interfere if shifted spikes merge into adjacent spike patterns. Whether this is a problem depends on two factors, namely (1) whether it is necessary to retrieve clear representations of individual items during tasks that depend on the retrieval of specific episodes, and (2) whether strong autoassociative encoding of individual items in other regions of the hippocampus can sufficiently correct the spiking representations that best match spike patterns in retrieved episodes.

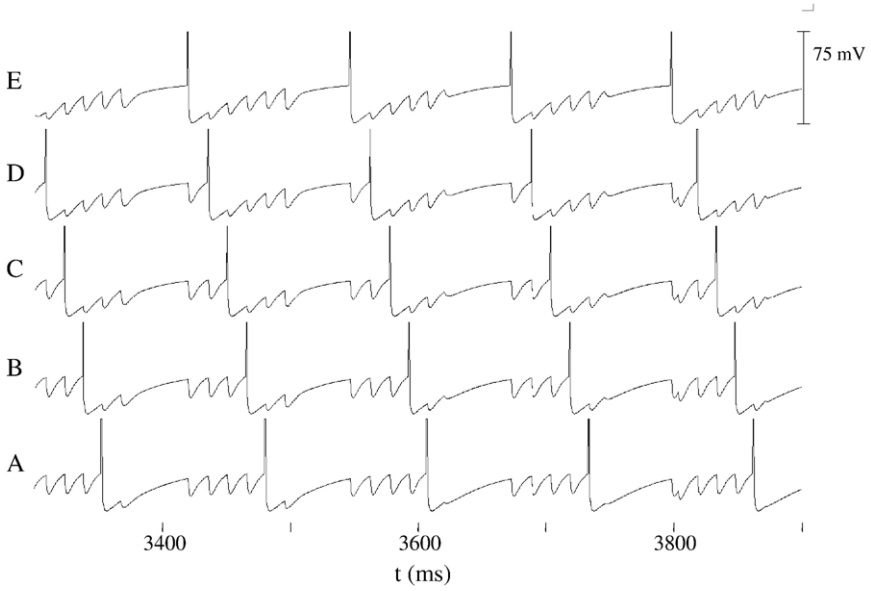

Fig. 6 – The membrane potential of one neuron in each of five reversed order buffered items (A to E), simulated with model pyramidal neurons that exhibit after-depolarization responses that span more than two theta cycles. The full simulation involved first-in first-out reversed order buffering of 15 items, each of which was represented by four spiking neurons.

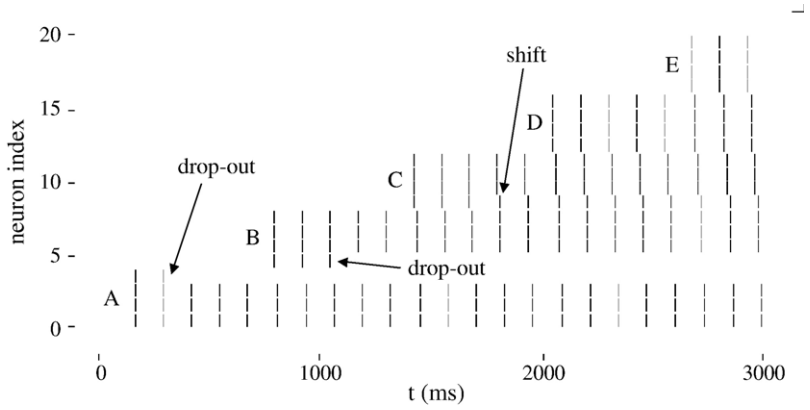

Fig. 7 – Simulated spike responses of five reversed order buffered item representations (A to E, with four spiking neurons each) in which pyramidal neurons were modeled with differences in the individual after-depolarization response rise time constant. Sustained spikes of neurons three and four drop-out ("drop-out" arrows). The sustained spikes of neuron eight, though initially elicited as part of the representation of the third item, become associated with the representation of the second item ("shift" arrow).

The effect of differences between the ADP parameters of individual pyramidal neurons in the same network is shown in Fig. 7:

1. Differences that amount to less than 15% of the ADP rise time constant (most neurons shown in Fig. 7) did not affect the participation of neurons in buffer function. Recurrent inhibition was strong enough to enforce synchronization.
2. A change of the ADP rise time constant from 140 ms to 90 ms (neuron 3) and 100 ms (neuron 4) was the first value at which the ADP did not last long enough for the neurons to participate in buffering for more than a few cycles. Reactivation ceased as new items settled into a specific theta phase, when the interval for persistent spiking is equal to a theta cycle. The intervals were smaller when a new item was still shifting from late phase to earlier phases.
3. A change of the ADP rise time constant from 140 ms to 160 ms (neuron 8) was the first value at which the ADP difference caused a shift of the reactivated spike into another gamma interval. As a consequence, the neuron was dropped from the representation of the third item, and recruited into the representation of the second item. Such desynchronization also occurred in simulations where some neurons had even larger ADP rise time constants.

The effect of differences between ADP time constants may be non-critical when the number of candidate spiking neurons that may participate in the buffered representation of an item is large enough. Participation is self-selective for suitable parameters during the initial cycles of item buffering. Synapses may then be strengthened between input cues and successful buffered spike patterns.

Changing the strength of recurrent inhibition or changing the frequency of theta rhythm directly affects buffer capacity. Lowering the theta frequency (Fig. 8A) increases the number of item representations that can be sustained in each cycle, but reduces the number of cycles and therefore repetitions within a

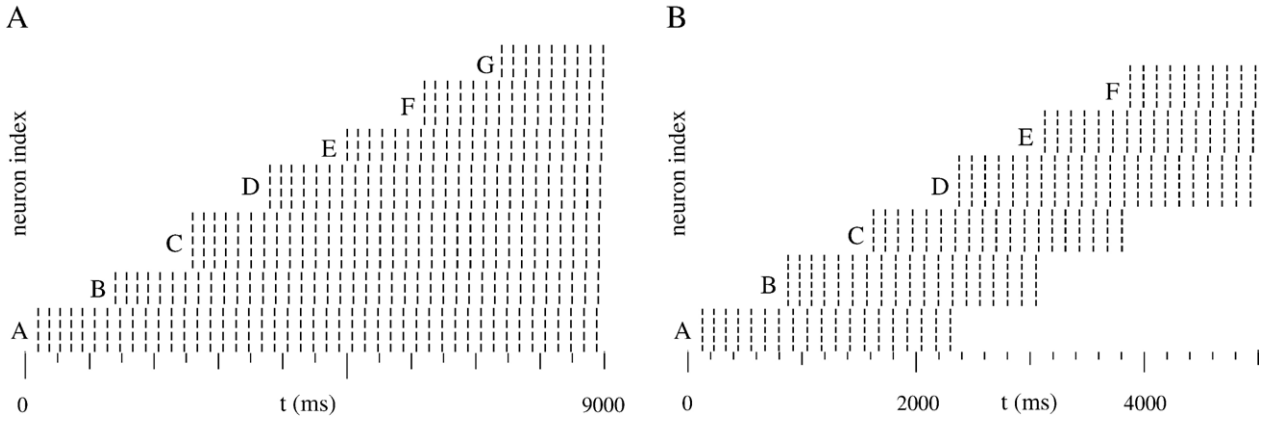

Fig. 8 – Simulated forward order buffering in models with modified theta and gamma intervals. (A) Reduced theta frequency in a simulation with seven consecutive items (A to G) represented by patterns of three to five spikes each (a total of 26 spiking neurons). The increased duration of the theta cycles was able to accommodate the sustained reactivation of all seven spike patterns. (B) Stronger network-wide recurrent "gamma" inhibition in a simulation with six items represented by patterns of five or six spikes each. Buffer capacity was reduced to three items.

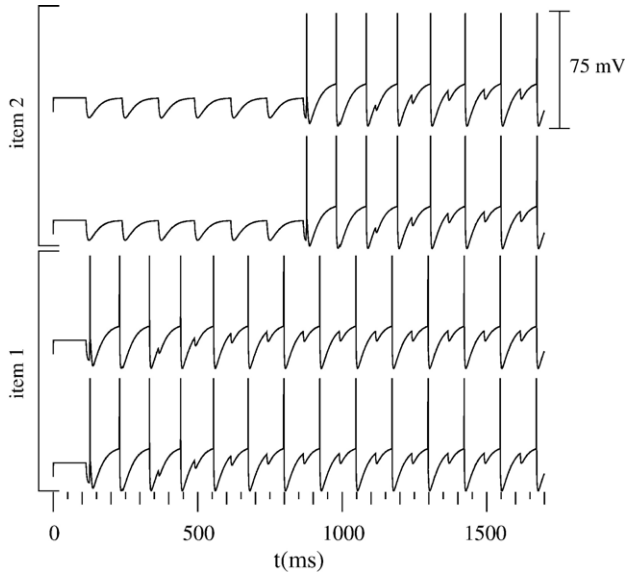

Fig. 9 – Membrane potential of pyramidal neurons in a simulated buffer with network-wide weak inhibition by "gamma" interneurons, with two items represented by two spiking neurons each. After about seven cycles of reactivation of the second buffered item representation, the two consecutive spike patterns merge into a single pattern of synchronous spikes. The membrane potential responses shown here were the result of a simulation with a buffer containing 32 persistent firing pyramidal cells, of which subsets of five or six spiking neurons represented six different items.

given time span. That reduction can proportionately affect the strength of encoding by STDP in recurrent networks of the hippocampus during that time span. Strengthening recurrent "gamma" inhibition (Fig. 8B) increases the time interval between sustained spike patterns, which decreases the number of buffered items that can be sustained in each cycle. Weakening recurrent inhibition (Fig. 9) increases that number, but buffer function breaks down if the inhibition is too weak to maintain adequate item separation, so that spike patterns representing consecutive items merge.

A network-wide theta rhythm may be assumed for ECII, yet the strength of recurrent inhibitory connections targeting individual pyramidal neurons may differ. We investigate consequences of such individual differences. When specific neurons experienced a 20% greater amplitude of recurrent inhibition (raised from 50 nS to 60 nS), their participation in item representations in a reversing buffer was not affected (Fig. 10A). Once that difference was changed to 50% (75 nS) in model neurons 3 and 4, neuron 4 exhibited reduced buffering capacity and dropped out once the buffer was presented with a third item. Neuron 3 was less affected, due to its later phase of reactivation.

When specific neurons experienced less inhibition (from 50 nS to 40 nS for neuron 3 and to 30 nS for neuron 4), the shorter period of inhibition may cause spikes of those neurons to shift to an earlier gamma interval of the buffer (Fig. 10B). As this occurs during the first cycles of item buffering, such shifts imply that the weakly inhibited neurons will not participate in item representations established by reliable coherence.

4. Discussion

Individual differences between the model parameters of buffer neurons may affect reliable buffer function and may affect the capacity of the buffer in terms of the number of spike patterns that may be sustained in short-term memory. At the system level, this capacity affects hippocampal encoding and retrieval of episodic memory. Buffer capacity determines how many items may be added to the buffer as spike pattern input until the first item is dropped from the queue. In spatial tasks, this determines the effective area of the place fields that may be associated with place cell activity elicited in the hippocampus (Fig. 11). In general, the ordinal distance across which connections between items in an episode may be strengthened during heteroassociative encoding is affected. As discussed below, the effective size of

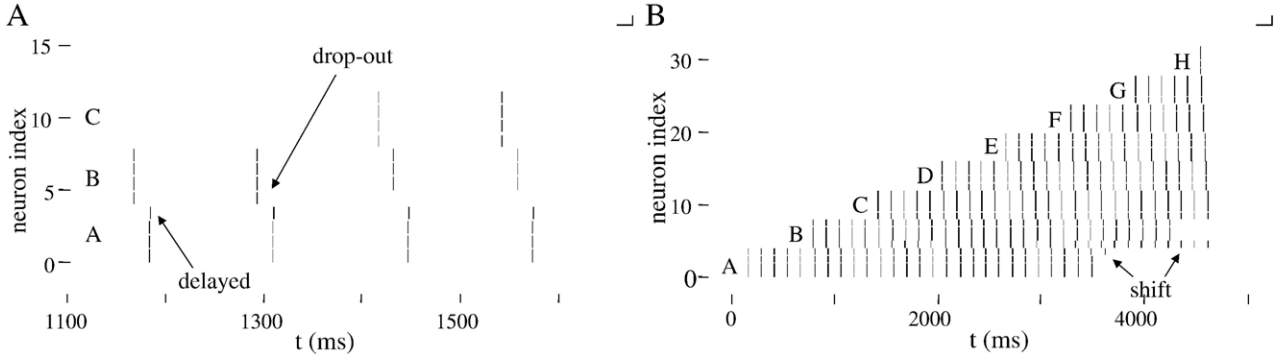

Fig. 10 – Spike responses during simulated reverse ordered buffering with differences between the strength of recurrent inhibition experienced by individual buffer neurons. (A) Three item representations (A to C) consisting of four spikes each, when some model neurons experience stronger "gamma" inhibition. Spiking of neuron three is delayed during buffer cycles between t=1100 ms and t=1500 ms ("delayed" arrow), but is then realigned. The difference of recurrent inhibition experienced by neuron four causes drop out of its spiking after t=1400 ms ("drop-out" arrow). (Note the difference in time scale compared to other figures.) (B) Eight item representations (A to H) consisting of four spikes each, when some model neurons experience weaker "gamma" inhibition. After t=3000 ms, the spiking neurons three and four become aligned and therefore associated with spike patterns sustaining items different than the two they had previously been aligned with ("shift" arrows).

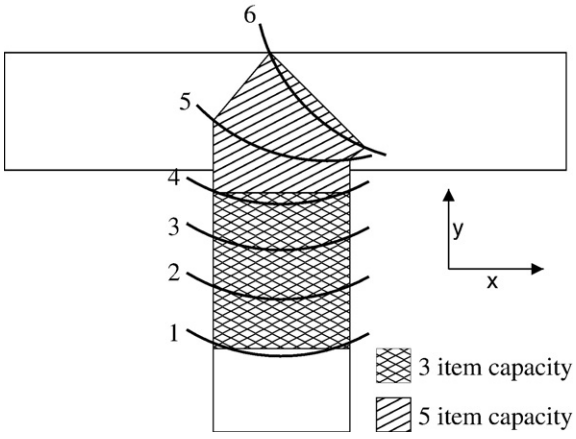

Fig. 11 – The relationship between effective hippocampal place fields and buffer capacity. Black curved lines indicate positions during a spatial task, at which the onset of spiking of a place cell (numbered 1 to 6) registers as input to ECII. Buffering that spike until three more input items are received results in the effective place field indicated by the cross-hatched area. If the spike is lost only after five more input items are received, then the effective place field is indicated by the cross-hatched plus right-diagonal area.

place fields established by the buffer capacity of ECII pyramidal neurons may through recurrent collaterals in ECII interact with grid activity of ECII stellate cells (Hafting et al., 2005).

Individual differences have two main consequences:

1. Subsets of neurons with similar parameters form functional categories. Input spikes may be sustained in multiple buffers with properties determined by the category of the participating neurons. During behavioral tasks, ECII may provide more than one short-term buffered representation of episodic activity to the hippocampal system. A significant example of useful multiple buffer resources are the forward order and reversed order buffer types, for which the neural mechanism differs only in terms of the delay with which input arrives at ECII neurons, the theta phase offset of novel input. In future work, we will investigate the parallel operation of multiple buffers, which in some cases may also involve establishing lateral innervation by separate groups of interneurons.
2. A neuron with different parameter values may not be able to participate in a specific item representation or may drop out after a few cycles. Neuron drop-out is also a common and gradually increasing consequence of noise. Spike drop-outs reduce the representing neuron ensemble size. When this reduction occurs gradually, due to the effects of noise in the buffer, the combined output spiking activity of representations for each buffered item is proportional to an item's age (the duration for which it has been sustained) in the buffer. A translation such as this, of the ordinal buffer position of an item (time-domain) to a corresponding activity level can be useful as a way to provide working memory of context (Howard and Kahana, 2002).

   A noisy persistent firing buffer with repeated sequence activity at theta rhythm is not the only proposed mechanism with which to achieve a distributed representation of temporal context. Sustained graded firing rates in layer V of EC (ECV) have been proposed as a useful mechanism to support the activity of such population-coded context representations (Fransén et al., 2006; Howard and Kahana, 2002). The graded firing rates shown to be sustained in ECV are not a suitable buffer for ordered spike sequences during heteroassociative encoding by STDP. By contrast, the regular spiking exhibited by ECII pyramidal neurons with ADP is very well suited to that purpose.

Large ensemble sizes can mitigate the functional consequences of parameter and noise related spike drop-out. ECII contains many neurons, and between tasks the resource can be recycled into new item representations. Nevertheless, the minimum reliable ensemble size does place a limit on the number of successful item representations that may be established and buffered in ECII during behavior. Unlike encoding in associative memory networks, overlapping representations are not desirable, since persistent spiking in ECII is specifically useful as a one-shot short-term memory for novel items. Existing recurrent fiber connections between pyramidal neurons in ECII may imply natural attractors that are expressed as neural ensembles with consistent coherent spiking. Such ensembles may form reliable and even pattern-completing representations when activated during the presentation of input to ECII.

As shown here and previously (Koene and Hasselmo, 2007), changing the duration of the theta cycles or of spike suppression by recurrent inhibition directly controls the capacity of the proposed buffer model. A greater duration of the ADP response can be accommodated readily in the reverse order form of the buffer, while the forward order buffer then requires a proportionally stronger inhibition to terminate items for first-in-first-out replacement. In future work, we will simulate the response dynamics of ECII pyramidal cells in more detail, and we will consider the causes of different realistic time constants of ADP that have been proposed by Fransén et al. (2002) and by Andrade (1991).

We speculate that the potential for multiple buffers with different item capacity limits supported by ECII pyramidal cell activity may interact with ECII stellate cell activity that exhibits grid-like place-dependent activity at different spatial grid frequencies (Hafting et al., 2005). The persistent firing could allow linking of specific item representations to active grid cells, or could perturb the spatial pattern of firing in a manner that influences context-dependent firing of place cells. The stellate cell output then projects to regions of the hippocampus, such as the dentate gyrus and region CA3 (Heinemann et al., 2000).

There are some functional limitations to the buffer model. Smaller intervals between successive retrieved spike patterns in the buffer enable buffering of longer sequences, but short-term buffer function deteriorates at recurrent inhibition strengths below G_{gamma}=2.5 nS, since the inhibition becomes insufficient to reliably separate item spike patterns when spike times are shifted by realistic noise. Recent studies of associations between changes in gamma frequency oscillations and effectiveness of encoding in humans provide a compelling justification for this limitation (Sederberg et al., 2007). It is plausible that strong gamma oscillations are needed to maintain item separation.

As implemented, the buffer model contains no direct recurrent connections between buffer pyramidal neurons.

Consequently, no attractor network functions, such as pattern completion, are possible without involving a separate recurrent network during retrieval. Item representations in the buffer automatically separate into distinct subsets of spiking pyramidal neurons. This leads to competing demands: On one hand, item spike patterns that involve a large number of neurons can more robustly buffer a sequences of item representation by noisy persistent firing. On the other hand, item patterns represented by large non-overlapping sets of neurons can limit the number of item representations that may be generated for a task.

Properties of the buffer model, specifically after-hyperpolarization and the functional "reset" of saturated ADP responses following a spike, necessitate a form of repetition blindness[2] for a specific context-dependent representation of item input that is identical to a buffered item (Koene, 2001, ch. 5). As spikes are dropped from the noisy representation of a buffered item, those spikes become available for renewed activation when place cell spikes continue to be elicited in large or non-sparse ECII place fields. Both a gradual decrease of item activity and a gradually renewed activity are therefore possible, which may be mirrored by the rate of stellate grid cell activity around grid nodes. Depending on the buffer capacity, the first buffered item will be replaced after a specific number of other place cell inputs are received, which correspond to overlapping place fields in ECII. If the current location is still within the spatial boundaries of many of the same large overlapping place fields, then input similar to that which elicited the recently replaced item may return to the buffer. This sequence of buffer events, via recurrent output to ECII stellate cells, can interact with the observed regular spacing of grid nodes with elevated spike rates and the low spike rate spaces between them.

Our model provides a robust short-term memory used to simulate behavioral tasks, especially those that depend on regular cycles of alternating encoding and retrieval of episodic memory (Hasselmo et al., 2002; Cannon et al., 2003; Koene et al., 2003; Koene and Hasselmo, 2005; McGaughy et al., 2005; Ergorul and Eichenbaum, 2006). The buffer model is also able to generate reversed order sequences that enable reversed heteroassociative encoding by STDP. Here, we examined the effect of differences in the values of significant model parameters. Significant effects resulted from differences in the time constants of the ADP response, from different phase offsets of afferent input spikes, from different theta frequencies, and from differences in the strength of recurrent inhibition. Relatively small differences between the parameter values of individual model neurons do not critically affect buffer function. Greater differences lead either to spike drop-out or to spikes that shift between adjacent item representations. Groups of many neurons in ECII with similar parameter values may function as parallel buffers with distinct properties.

Previously (Koene and Hasselmo, 2007), we described a possible connection between the optimal separation of buffered items by recurrent inhibition for robust buffer operation, as first proposed by Lisman and Idiart (1995), and a 4±1 short-term memory capacity limit espoused by Cowan (2001). Present results suggest that ECII may provide resource subsets for multiple buffers with different characteristics in terms of item separation, buffer capacity, and sequence order, mechanistic differences that may be involved in the category-dependent and chunking-dependent differences of measured short-term memory capacity (Wickens, 1984; Daneman and Merikle, 1996).

Self-selection of appropriate resources in terms of neurons with similar characteristic model parameter values may be the main mechanism to assure adequate buffer operation. Such selective appropriation is a cheap solution in evolutionary terms, since the plentiful production of neurons and synapses in ECII is a straightforward developmental step. Neurons with similar parameters can provide buffer function with group-specific properties. Grouping is further aided by the existence of a priori recurrent connections in the network of pyramidal neurons in ECII. We will investigate self-selection in future work, which will require simulating hundreds of ECII model neurons.

[2] The neural mechanism that may accomplish "novelty detection" in the hippocampal system is often thought to involve a comparison function in CA1 (Lisman, 1999).

Acknowledgments

The CATACOMB simulations described here and information about the CATACOMB environment created and maintained by Robert C. Cannon are available on our Computational Neurophysiology Web site at http://askja.bu.edu.

Supported by NIH R01 grants DA16454 (CRCNS), MH60013, and MH61492 to Michael Hasselmo, by the NSF Science of Learning Center SBE 0354378 and NIMH Silvio O. Conte Center grant MH71702.

Appendix A

For the simulations presented here, the short-term buffer model was implemented with leaky integrate-and-fire neurons, in which an explicit membrane capacitance determines the time-constant of exponential decay to resting potential. The membrane potential of all modeled neurons and interneurons is modulated by rhythmic input at a theta frequency of 8 Hz, synaptic input, intrinsic after-hyperpolarization, and a leak current. The theta modulation is introduced to the neurons through inhibitory synaptic input that is driven by an abstracted model of fibers propagating activity from the medial septum. In addition to this, the modeled pyramidal neurons of layer II of entorhinal cortex that are supposed to sustain persistent firing experience after-depolarization. The conductance response of each of these currents is described by a double-exponential function,

$$g_i(t) = G_i a_{norm}(\exp(-t/\tau_{fall,i}) - \exp(-t/\tau_{rise,i})), \quad (1)$$

where G_i is the characteristic amplitude of the conductance response for a specific membrane current, and $\tau_{fall,i}$ and $\tau_{rise,i}$ are its fall and rise time constants. A normalizing factor a_{norm} is used to insure that the maximum value of $g_i(t)$ is G_i,

$$a_{norm} = 1/(\exp(-t_{max}/\tau_{fall,i}) - \exp(-t_{max}/\tau_{rise,i})), \quad (2)$$

with the time offset of the maximum response value,

$$t_{max} = \ln\left\{\frac{\tau_{fall,i}/\tau_{rise,i}}{(1/\tau_{rise,i}) - (1/\tau_{fall,i})}\right\}. \quad (3)$$

Table 1 – Default parameter values of modeled membrane currents in the short-term buffer simulations

Membrane current	τ_{rise} (ms)	τ_{fall} (ms)	G (nS)	E_{rev} (mV)
Pyramidal buffer neurons				
After-hyperpolarization	10^{-4}	30	23	−90
After-depolarization	125	125	30	−45
Asymmetric theta modulation	0.1	20	10	−90
Input from "gamma" interneuron	0.1	2.5	100	−70
Leak		9	111	−60
"Gamma" interneuron				
After-hyperpolarization	10^{-4}	4	100	−90
Input from buffer pyramidal neurons	1	2	30	0
Leak		10	100	−70

Leak currents are modeled as exponential decay functions to resting potential, and therefore have only one time constant. Leak conductance is related to the leak time constant by $G_{leak}=C/\tau_{leak}$.

Computed individual time-specific conductance values $g_i(t)$ determine contributions to the change Δv of the membrane potential V during a small time interval Δt,

$$\Delta v = \frac{\sum_i (g_i \Delta t (E_{rev,i} - V))}{C + \sum_i (g_i \Delta t)}, \quad (4)$$

where $C=1$ mF is the membrane capacitance and $E_{rev,i}$ the reversal potential of a contributing membrane current. The firing threshold is −50 mV. The pyramidal neuron resting potential is −60 mV, and the interneuron resting potential is −70 mV. Action potentials have a duration of 1 ms and followed by a 2 ms refractory period and by after-hyperpolarization. The default parameter values used in simulations were introduced in Koene and Hasselmo (2007) and are shown in Table 1. The recurrent connectivity in the buffer network is such that the interneuron representing interneuron network activity receives input from all pyramidal buffer neurons and sends spike output to all pyramidal buffer neurons.

In simulations with noise, noise was added through simulated current clamps of individual neurons driven by a first order autoregressive process (a model for the response to noise that is similar to a random walk) with Poisson distribution, a mean value of 0, an amplitude of 1 pA, and a regression parameter of 0.5. Strong noise had amplitude values up to ±10 pA, and very strong noise had amplitude values between ±60 and ±70 pA.

In Fig. 12, we show interacting specialized pyramidal neurons and interneurons that demonstrate that a first-in first-out item replacement function is possible in the forward order persistent firing buffer model. The mechanism demonstrated was introduced in Koene and Hasselmo (2007).

Symbolic units simplify the description of the replacement mechanism in Fig. 12. The P_{ADP} unit is a superposition of all the pyramidal buffer neurons that spike persistently, due to an intrinsic mechanism such as after-depolarization. The units Pf and Pi are simplified representations of two ensembles of pyramidal neurons that do not exhibit intrinsic spiking. The ensemble represented by Pi receives external input. The ensemble represented by Pf receives feedback from the intrinsically spiking pyramidal buffer neurons. The Pf and Pi units were implemented in the model network as two individual pyramidal neurons. Similarly, the Ir unit represents an ensemble of interneurons that is driven separately from those interneurons responsible for inhibition at gamma intervals. The Ir unit was implemented as a single interneuron receiving input from the neuron implementations of the Pf and Pi units.

The trace of the symbolic P_{ADP} unit shows when any of the pyramidal neurons in the buffer that experience intrinsic after-depolarization reactivate to maintain item spike patterns. Septal input at theta frequency modulates the membrane potential of

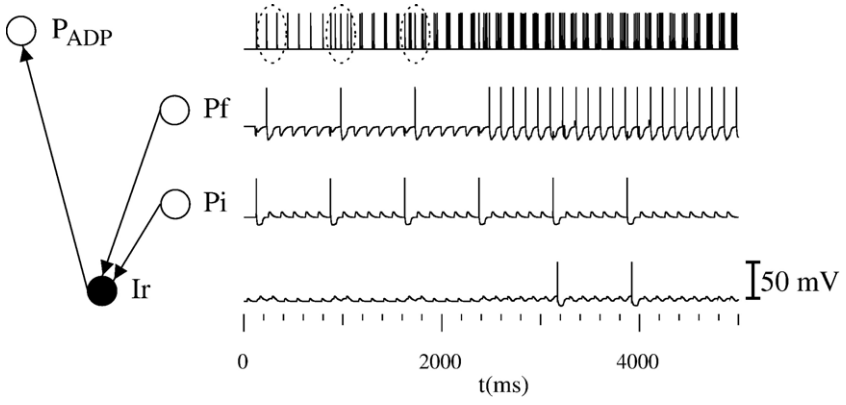

Fig. 12 – Simulated responses of the membrane potential of specialized populations of pyramidal neurons and interneurons that may interact to elicit first-in first-out item replacement in a persistent firing short-term buffer. The P_{ADP} unit shown represents the combined activity of all intrinsic spiking pyramidal neurons in our model of layer II of entorhinal cortex. The Pf unit represents pyramidal neurons that activate once during each theta cycle in which the buffer is filled to capacity, while the Pi unit represents pyramidal neurons that activate once during each theta cycle in which afferent input elicits activity in the buffer. Dotted circles indicate the buffer activity during three spurious "full buffer" spikes. The Ir unit represents interneurons that receive input from Pf and Pi neurons. Ir spikes exert replacement inhibition at P_{ADP} buffer pyramidal neurons. The response trace of Ir interneurons shows two occasions that elicit replacement inhibition spikes, namely when the fifth and sixth afferent input stimuli appear.

Pf (full buffer detecting) and Pi (buffer input detecting) neurons at the same phase as the membrane potential of buffer neurons represented in the P_{ADP} trace.

The neural mechanism shown is tuned to a forward-order buffer with a sequence capacity of four items. The efficacy of transmission through output connections from buffer neurons (represented by P_{ADP}) to Pf neurons is modulated at theta frequency, to strongly transmit only spikes at the theta phase interval of a reactivated fourth item in the buffer. If a fourth item is reactivated in the buffer, then Pf neurons spike. Spurious "full buffer" spikes in Fig. 12 (spikes in Pf below dotted ellipses) occur immediately after first, second, and third item afferent input stimulation. In those cases, reactivated item spikes have yet to shift into earlier phases of the theta cycle.

The output of Pf and Pi neurons converges at specialized interneurons (Ir). Septal input at theta frequency modulates the membrane potential of the interneurons, effectively imposing a phase-lock on the timing of possible spikes elicited at Ir. The combination of full buffer and afferent input signals therefore elicits theta phase synchronized spikes of the Ir interneurons. The phase-lock ensures that Ir activity inhibits activity at the phase of first item reactivation in the short-term buffer. First item reactivation is tuned to be possible only at the maximum depolarization by the combination of theta modulation and ADP at that phase. Consequently, the interval of suppression by "replacement inhibition" causes termination of the persistent first item spike pattern.

REFERENCES

Acker, C., Kopell, N., White, J., 2003. Synchronization of strongly coupled excitatory neurons: relating network behavior to biophysics. J. Comput. Neurosci. 15 (1), 71–90.

Andrade, R., 1991. The effect of carbachol which affects muscarinic receptors was investigated in prefrontal layer v neurons. Brain Res. 541, 81–93.

Atkinson, R., Shiffrin, R., 1968. Human memory: a proposed system and its control processes. In: Spence, K., Spence, J. (Eds.), The Psychology of Learning and Motivation, vol. 2. Academic Press, New York, pp. 89–105.

Bi, G., Poo, M., 1998. Synaptic modifications in cultured hippocampal neurons: dependence on spike timing, synaptic strength, and postsynaptic cell type. J. Neurosci. 18 (24), 10464–10472.

Cannon, R., Hasselmo, M., Koene, R., 2003. From biophysics to behaviour: Catacomb2 and the design of biologically plausable models for spatial navigation. Neuroinformatics 1 (1), 3–42.

Cowan, N., 2001. The magical number 4 in short-term memory: a reconsideration of mental storage capacity. Behav. Brain Sci. 24 (1), 84–114.

Crowder, R., Morton, J., 1969. Precategorical acoustic storage (pas). Percept. Psychophys. 5, 365–373.

Daneman, M., Merikle, P., 1996. Working memory and language comprehension: a meta-analysis. Psychon. Bull. Rev. 3, 422–433.

Egorov, A., Hamam, B., Fransen, E., Hasselmo, M., Alonso, A., 2002. Graded persistent activity in entorhinal cortex neurons. Nature 420 (6912), 173–178.

Ergorul, C., Eichenbaum, H., 2006. Essential role of the hippocampal formation in rapid learning of higher-order sequential associations. J. Neurosci. 26 (15), 4111–4117.

Foster, D., Wilson, M., 2006. Reverse replay of behavioural sequences in hippocampal place cells during the awake state. Nature 440, 680–683.

Fransén, E., Alonso, A., Hasselmo, M., 2002. Simulations of the role of the muscarinic activated calcium-sensitive nonspecific cation current i_{NCM} in entorhinal neuronal activity during delayed matching tasks. J. Neurosci. 22 (3), 1081–1097.

Fransén, E., Tahvildari, B., Egorov, A., Hasselmo, M., Alonso, A., 2006. Mechanism of graded persistent cellular activity of entorhinal cortex layer V neurons. Neuron 49, 735–746.

Giocomo, L., Zilli, E., Fransen, E., Hasselmo, M., 2007. Temporal frequency of subthreshold oscillations scales with entorhinal grid cell field spacing. Science 315, 1719–1722.

Haarmann, H., Usher, M., 2001. Maintenance of semantic information in capacity-limited item short-term memory. Psychon. Bull. Rev. 8 (3), 568–578.

Hafting, T., Fyhn, M., Molden, S., Moser, M.B., Moser, E., 2005. Microstructure of a spatial map in the entorhinal cortex. Nature 436, 801–806.

Hasselmo, M., Cannon, R., Koene, R., 2002. A simulation of parahippocampal and hippocampal structures guiding spatial navigation of a virtual rat in a virtual environment: a functional framework for theta theory. In: Witter, M., Wouterlood, F. (Eds.), The Parahippocampal Region: Organization and Role of Cognitive Functions. Oxford University Press, Oxford, pp. 139–161.

Hebb, D., 1949. The Organization of Behavior. Wiley, New York.

Heinemann, U., Schmitz, D., Eder, C., Gloveli, T., 2000. Properties of entorhinal cortex projection cells to the hippocampal formation. Ann. N.Y. Acad. Sci. 911, 112–126.

Howard, M., Kahana, M., 2002. A distributed representation of temporal context. J. Math. Psychol. 46 (3), 269–299.

Jacobs, J., Kahana, M., Ekstrom, A., Fried, I., 2007. Brain oscillations control timing of single-neuron activity in humans. J. Neurosci. 27 (14), 3839–3844.

Jensen, O., Idiart, M., Lisman, J., 1996. Physiologically realistic formation of autoassociative memory in networks with theta/gamma oscillations: role of fast NMDA channels. Learn. Memory 3, 243–256.

Johnson, A., Redish, A., 2006. Neural ensembles in CA3 transiently encode paths forward of the animal at a decision point: a possible mechanism for the consideration of alternatives. 2006 Neuroscience Meeting Planner. Society for Neuroscience, Atlanta, GA. Online.

Kahana, M., 1996. Associative retrieval processes in free recall. Mem. Cogn. 24 (1), 103–109.

Klink, R., Alonso, A., 1997a. Morphological characteristics of layer ii projection neurons in the rat medial entorhinal cortex. Hippocampus 7, 571–583.

Klink, R., Alonso, A., 1997b. Muscarinic modulation of the oscillatory and repetitive firing properties of entorhinal cortex layer ii neurons. J. Neurophysiol. 77 (4), 1813–1828.

Koene R., 2001. Functional requirements determine relevant ingredients to model for on-line acquisition of context dependent memory. PhD. thesis, Department of Psychology, McGill University, Montreal, Canada.

Koene, R., Hasselmo, M., 2005. An integrate and fire model of prefrontal cortex neuronal activity during performance of goal-directed decision making. Cereb. Cortex 15 (12), 1964–1981 Advanced Access published on April 27, 2005.

Koene, R., Hasselmo, M., 2006a. An integrate-and-fire model of temporal context specific episodic encoding and retrieval in the hippocampal formation. Proceedings of the Computational and Systems Neuroscience (COSYNE) Meeting 2006, p. 80. Salt Lake City, UT. (#90).

Koene, R., Hasselmo, M., 2006b. A model of reverse reactivation of episodic activity in the hippocampus during idle awake periods. 2006 Neuroscience

Meeting Planner. Society for Neuroscience, Atlanta, GA. Online.
Koene, R., Hasselmo, M., 2007. First-in-first-out item replacement in a model of short-term memory based on persistent spiking. Cereb. Cortex. 17 (8), 1766–1781.
Koene, R., Gorchetchnikov, A., Cannon, R., Hasselmo, M., 2003. Modeling goal-directed spatial navigation in the rat based on physiological data from the hippocampal formation. Neural Netw. 16 (5–6), 577–584.
Lisman, J., 1999. Relating hippocampal circuitry to function: recall of memory sequences by reciprocal dentate-CA3 interactions. Neuron 22, 233–242.
Lisman, J., Idiart, M., 1995. Storage of 7±2 short-term memories in oscillatory subcylces. Science 267, 1512–1515.
McGaughy, J., Koene, R., Eichenbaum, H., Hasselmo, M., 2005. Cholinergic deafferentation of the entorhinal cortex in rats impairs encoding of novel but not familiar stimuli in a delayed nonmatch-to-sample task. J. Neurosci. 25 (44), 10273–10281.
Sederberg, P., Schulze-Bonhage, A., Madsen, J., Bromfield, E., McCarthy, D., Brandt, A., Tully, M., Kahana, M., 2007. Hippocampal and neocortical gamma oscillations predict memory formation in humans. Cereb. Cortex 17 (5), 1190–1196.
White, J., Rubinstein, J., Kay, A., 2000. Channel noise in neurons. Trends Neurosci. 23, 131–137.
Wickens, C, 1984. Processing resources in attention. In: Parasuraman, R., Davies, D. (Eds.), Varieties of Attention. Academic Press, New York, pp. 63–102.